

## Polarization scrambling in Brillouin optical correlation-domain reflectometry using polymer fibers

Neisei Hayashi, Kazunari Minakawa, Yosuke Mizuno, and Kentaro Nakamura

*Precision and Intelligence Laboratory, Tokyo Institute of Technology, Yokohama 226-8503, Japan*

Received March 26, 2015; accepted April 19, 2015; published online May 13, 2015

We evaluate whether the measurement stability of Brillouin optical correlation-domain reflectometry (BOCDR) using polymer optical fibers (POFs) can be enhanced by polarization scrambling. In this study, two major factors that affect the signal-to-noise ratio in BOCDR, specifically, the spatial resolution and incident power, are varied, and their influences on distributed measurements with polarization scrambling are experimentally investigated. We thus confirm that in POF-based BOCDR, unlike in BOCDR using standard silica glass fibers, polarization scrambling is an effective means of enhancing the measurement stability only when the spatial resolution is sufficiently low or when the incident power is sufficiently high. © 2015 The Japan Society of Applied Physics

For the past several decades, increasing attention has been directed toward Brillouin scattering in optical fibers,<sup>1)</sup> which can be used to develop lasers,<sup>1)</sup> microwave signal processors,<sup>2)</sup> optical memories,<sup>3)</sup> phase conjugators,<sup>4)</sup> and slow-light generators.<sup>5)</sup> Strain and temperature sensors<sup>6–10)</sup> are also promising applications of Brillouin scattering due to its ability to measure the strain and temperature distributions along optical fibers. To date, the heads of Brillouin sensors have been composed mainly of glass optical fibers including silica single-mode fibers (SMFs), which, however, lack flexibility and cannot withstand strains of over ~3%. One promising solution to this drawback is to employ polymer optical fibers (POFs),<sup>11,12)</sup> which are highly flexible and can withstand large strains of over several tens of percent. Another advantage of POF-based sensors is a unique function called a “memory effect”,<sup>13)</sup> with which the information on the applied large strain can be stored by their plastic deformation.

Previous studies on Brillouin scattering in POFs<sup>14–17)</sup> have revealed that this phenomenon can potentially be used as a mechanism of large-strain sensing<sup>16)</sup> and of highly sensitive temperature sensing with less sensitivity to strain.<sup>17)</sup> Actual distributed Brillouin measurements using POFs were obtained by three research groups almost simultaneously in 2014. Minardo et al.<sup>18)</sup> employed Brillouin optical frequency-domain analysis (BOFDA)<sup>8,19)</sup> and examined a 4.0-m-long heated section (located at the edge) of a 20-m-long POF. The spatial resolution and signal-to-noise ratio (SNR) were, however, not sufficiently high for practical use. Dong et al.<sup>20)</sup> employed Brillouin optical time-domain analysis (BOTDA)<sup>7)</sup> and investigated the evolution of mode coupling with 3.3 m spatial resolution along a 40-m-long POF. They observed significant fluctuations of the Brillouin frequency shift (BFS) along the POF, a characteristic that is unique to pump–probe-based systems, including BOTDA, indicating the difficulty in using the current BOTDA system to measure the strain/temperature distributions along POFs. On the other hand, our group<sup>21)</sup> employed Brillouin optical correlation-domain reflectometry (BOCDR)<sup>10)</sup> and investigated a 10-cm-long heated section of a 1.3-m-long POF with a theoretical spatial resolution of 6.0 cm.

In BOCDR using a glass optical fiber, polarization scrambling<sup>22,23)</sup> is often employed to suppress the polarization-dependent signal fluctuations and to enhance the stability of long-term monitoring and of distributed measurements along the entire length of the fiber under test (FUT).<sup>24)</sup>

In contrast, all distributed measurements using POF-based BOCDR have been performed without polarization scrambling, in other words, with an optimized polarization state (strictly speaking, a relative polarization state between Brillouin Stokes and reference light beams).<sup>21)</sup> The measurements have been conducted in this manner because, in a POF with a BFS ~4 times lower than that in a silica SMF, the Rayleigh wing is raised and overlaps the Brillouin gain spectrum (BGS) by averaging the polarization state,<sup>25)</sup> leading to significant deterioration of the SNR of the Brillouin measurement. The lowered SNR is likely to induce fatal measurement errors in POF-based BOCDR, because the Brillouin signal in a POF is much weaker than that in a silica SMF due to the large core diameter and multimode nature.<sup>14)</sup> However, in long-term monitoring using POF-based BOCDR, polarization-dependent signal fluctuations need to be mitigated (an entire-length but fast measurement along a short POF does not suffer from the signal fluctuations).

In this work, we experimentally evaluated whether the measurement stability of POF-based BOCDR can be enhanced by polarization scrambling. In general, major factors that affect the SNR in BOCDR are the spatial resolution, incident pump power, and propagation loss (i.e., sensing position). Among these three, the influences of the first two factors were investigated; a 1.0-m-long section (position fixed) of a 3.0-m-long POF was heated. When the incident power was fixed at 31 dBm, distributed measurement with a spatial resolution of 0.67 m was feasible even with polarization scrambling, whereas that with a resolution of 0.45 m failed unless the polarization state was optimized. Furthermore, when the spatial resolution was fixed at 0.67 m, distributed measurement with an incident power of 27 dBm was feasible even with polarization scrambling, whereas that with an incident power of 23 dBm needed to be performed with an optimized polarization state. These results indicate that polarization scrambling can be exploited to enhance the measurement stability of POF-based BOCDR only when the spatial resolution is sufficiently low or when the incident power is sufficiently high.

BOCDR<sup>10,26)</sup> is known to be a Brillouin-based distributed sensing technique with intrinsic one-end accessibility and high spatial resolution. Its operating principle is based on the correlation control of continuous light waves in a self-heterodyne scheme. In other words, the pump and reference lights [instead of the probe light used in Brillouin optical correlation-domain analysis (BOCDA)<sup>9)</sup>] are sinusoidally

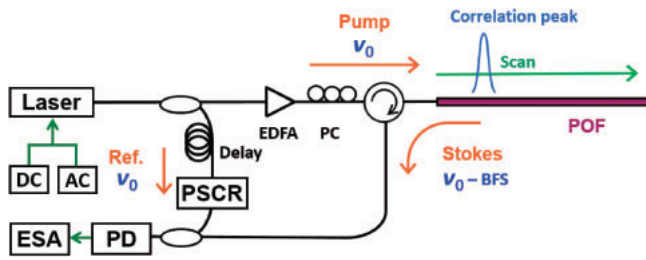


**Fig. 1.** Schematic setup of BOCDR containing PSCR in the reference path. AC, alternating current; DC, direct current; EDFA, erbium-doped fiber amplifier; ESA, electrical spectrum analyzer; PC, polarization controller; PD, photo detector.

frequency-modulated at  $f_m$ , with “correlation peaks”<sup>27)</sup> generated periodically along the FUT. The measurement range  $d_m$  is determined by their interval, which is inversely proportional to  $f_m$  as<sup>26)</sup>

$$d_m = \frac{c}{2nf_m}, \quad (1)$$

where  $c$  is the light velocity in a vacuum and  $n$  is the refractive index of the fiber core. By sweeping  $f_m$ , the correlation peak (namely, the sensing position) can be scanned along the FUT to acquire BGS and BFS distributions. The spatial resolution  $\Delta z$  is given by<sup>26)</sup>

$$\Delta z = \frac{c\Delta\nu_B}{2\pi n f_m \Delta f}, \quad (2)$$

where  $\Delta f$  is the modulation amplitude of the optical frequency and  $\Delta\nu_B$  is the Brillouin bandwidth. In a basic configuration, the upper limit of  $\Delta f$  is half the BFS of the FUT due to the inevitable noise caused by Rayleigh scattering.<sup>10,26)</sup>

As an FUT, we employed a 3.0-m-long perfluorinated graded-index POF<sup>27)</sup> with a numerical aperture of 0.185, core diameter of 50  $\mu\text{m}$ , cladding diameter of 70  $\mu\text{m}$ , overcladding diameter of 490  $\mu\text{m}$ , core refractive index of  $\sim 1.35$ , and propagation loss of  $\sim 250$  dB/km at 1.55  $\mu\text{m}$ . The core/cladding layers and overcladding layer were composed of amorphous perfluorinated polymer and polycarbonate,<sup>28)</sup> respectively.

A schematic setup of POF-based BOCDR is depicted in Fig. 1, which is essentially identical to that previously reported,<sup>10)</sup> except for some devices used to control the polarization state.<sup>24)</sup> All the optical paths excluding the FUT were silica SMFs. One end of the FUT was butt-coupled to the end of the second port of an optical circulator.<sup>14)</sup> The output from a distributed-feedback laser diode at 1.55  $\mu\text{m}$  with 1 MHz linewidth was sinusoidally frequency-modulated by direct modulation of the driving current. It was divided into two light beams with an optical coupler; one was guided through a 1-km-long delay fiber to adjust the correlation peak order and a polarization scrambler (PSCR) to switch on/off the average function of the polarization state. It was then used as the reference light of heterodyne detection (here, the “polarization state” means, in a precise sense, the relative polarization state between the Brillouin Stokes and reference light beams). The other beam was amplified with an erbium-doped fiber amplifier (EDFA), polarization-adjusted with a polarization controller (PC), and then injected into the POF as the pump light. Subsequently, the optical beat signal of the

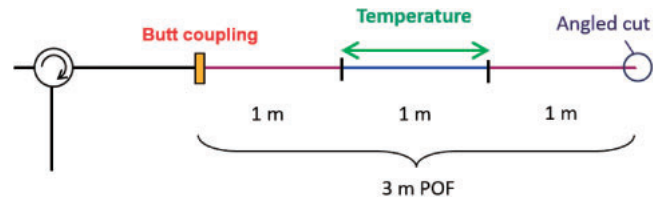


**Fig. 2.** Structure of tested POF.

Stokes and reference lights was converted to an electrical signal with a photo detector (PD) and was finally monitored as BGS with an electrical spectrum analyzer (ESA) with a 300 kHz frequency resolution.

As stated above, polarization scrambling in POF-based BOCDR drastically deteriorates the signal-to-noise ratio (SNR) of the measurement. To evaluate its influence, we first show that, when polarization scrambling is employed and the incident pump power is fixed, there exists a threshold spatial resolution, above which distributed measurements cannot be properly performed. The modulation frequency  $f_m$  was swept from 35.002 to 35.198 MHz, corresponding to the measurement range  $d_m$  of 3.2 m [see Eq. (1)]. The modulation amplitude  $\Delta f$  was set to 0.227 and 0.151 GHz, corresponding to nominal spatial resolutions  $\Delta z$  of 0.45 and 0.67 m [see Eq. (2); the Brillouin bandwidth  $\Delta\nu_B$  is reported to be  $\sim 100$  MHz<sup>14)</sup> in POFs]. The incident power was fixed at 31 dBm, and the polarization state was scrambled. The order of the correlation peak used for the measurement was 167, and the overall sampling rate of single-location BGS acquisition was 3.3 Hz. The room temperature was 18  $^\circ\text{C}$ . Figure 2 shows the structure of the FUT, where a 1.0-m-long section (position fixed) of a 3.0-m-long POF was heated to 45  $^\circ\text{C}$ .

Figures 3(a) and 3(b) show the normalized BGS distributions measured with 0.67 and 0.45 m spatial resolutions, respectively, and their BFS distributions are plotted in Fig. 3(c). The BFS in the unheated section was 2.83 GHz, which agreed well with the previously reported value.<sup>14)</sup> With 0.67 m resolution, the 1.0-m-long heated section was clearly detected and was determined to have an average BFS value of  $\sim 2.73$  GHz, which is reasonable considering that the temperature-dependence coefficient of the BFS is  $-3.2$  MHz/K.<sup>29)</sup> The measurement error (standard deviation) was calculated to be  $\sim \pm 1.0$   $^\circ\text{C}$ . In contrast, with 0.45 m resolution, the heated section was not properly detected because the raised Rayleigh wing overlapped with the BGS from lower frequencies, unlike in the case of silica-SMF-based BOCDR. This result indicates that there is a threshold spatial resolution between 0.45 and 0.67 m (precise determination is difficult due to the signal fluctuations) and that measurements with resolutions higher than the threshold cannot be performed with polarization scrambling.

Next, we demonstrated that, when polarization scrambling is employed and the spatial resolution is fixed, there exists a threshold incident pump power, below which distributed measurements fail. Figures 4(a), 4(b), and 4(c) show the BGS distributions with incident powers of 27, 23, and 20 dBm, respectively, and their BFS distributions are summarized in Fig. 4(d). The nominal spatial resolution was fixed at 0.67 m. The heated section was clearly detected with 27 dBm incident power, while the overlap of the raised Rayleigh wing disturbed proper detection of the heated section with 23

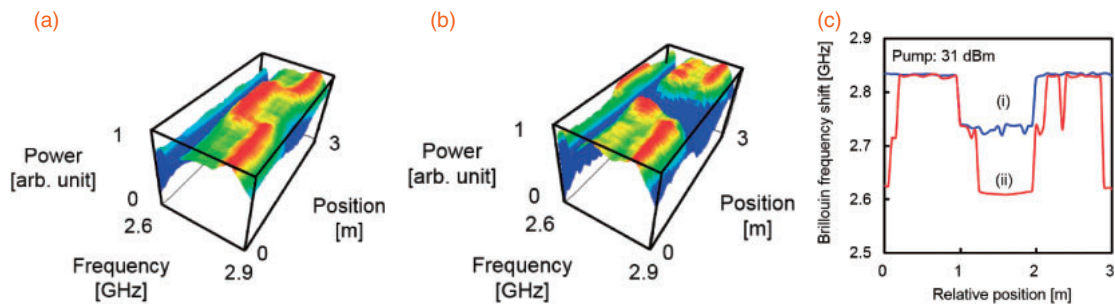


**Fig. 3.** Normalized BGS distributions measured with nominal spatial resolutions of (a) 0.67 and (b) 0.45 m. (c) BFS distributions with resolutions of (i) 0.67 and (ii) 0.45 m. Polarization state was scrambled.

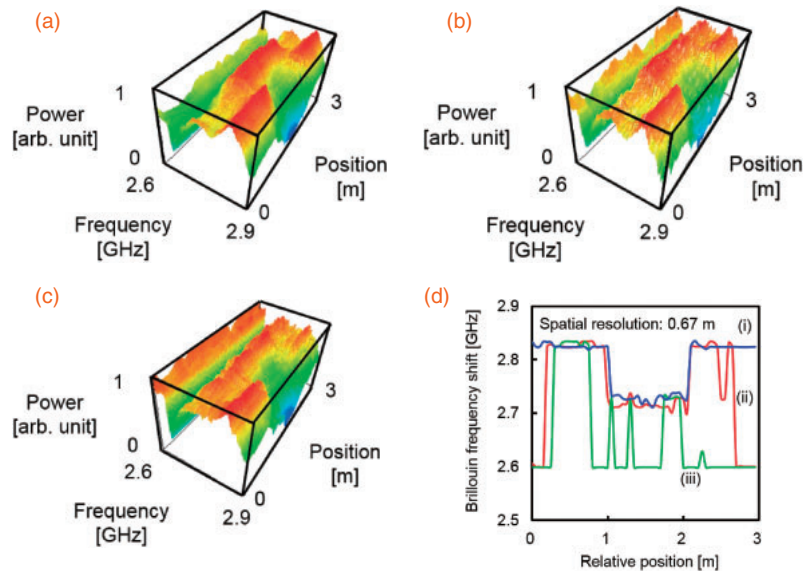


**Fig. 4.** Normalized BGS distributions with incident powers of (a) 27, (b) 23, and (c) 20 dBm. (d) BFS distributions with incident powers of (i) 27, (ii) 23, and (iii) 20 dBm. Polarization state was scrambled.

and 27 dBm incident powers. Thus, the threshold incident power was verified to lie between 23 and 27 dBm under these measurement conditions.

Finally, we confirmed that, when the polarization state is scrambled, the SNR of the measurement is deteriorated compared to that when the polarization state is optimized. Figure 5(a) shows the BFS distribution measured when the incident power was fixed at 31 dBm (same as in Fig. 3) and the spatial resolution was set to 0.38 m ( $< 0.45$  m;  $\Delta f$  was set to 0.269 GHz). The heated section was successfully detected. In addition, Fig. 5(b) shows the BFS distributions measured when the spatial resolution was fixed at 0.67 m (same as in Fig. 4) and the incident power was set to 23, 20, and 19 dBm. The heated section was properly detected with 23 dBm power, but detection failed at 20 and 19 dBm powers, indicating that the threshold power is lower than 23 dBm. These results clearly suggest that polarization scrambling lowers the SNR of the measurement compared to that when the polarization state is optimized; in other words, polarization scrambling enhances the long-term measurement stability at the cost of SNR deterioration and should be used with sufficiently low spatial resolution and sufficiently high incident pump power.

In conclusion, we experimentally investigated the influence of polarization scrambling on measurements by POF-based BOCDR. The spatial resolution and incident pump

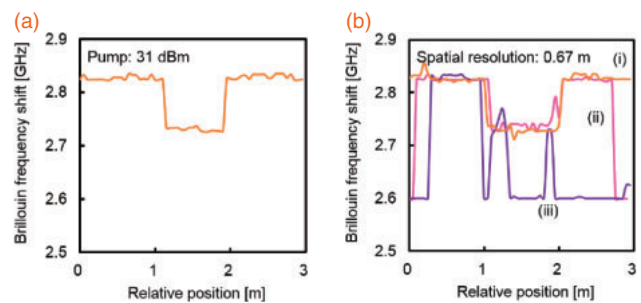


**Fig. 5.** (a) BFS distribution measured with 0.38 m spatial resolution. (b) BFS distributions with incident powers of (i) 23, (ii) 20, and (iii) 19 dBm. Polarization state was optimized.

power, which significantly affect the SNR, were varied, and their influences on the distributed measurements with polarization scrambling were evaluated. A 1.0-m-long section (position fixed) of a 3.0-m-long POF was heated. When the incident power was fixed at 31 dBm, distributed measurement with a spatial resolution of 0.67 m was successfully performed even with polarization scrambling, while that with a resolution of 0.45 m proved unsuccessful unless the polarization state was optimized. Meanwhile, when the spatial resolution was fixed at 0.67 m, distributed measurement with an incident power of 27 dBm was successfully conducted even with polarization scrambling, but that with an incident

power of 23 dBm had to be performed with an optimized polarization state. These results indicate that, unlike the case of silica-SMF-based BOCDR, polarization scrambling can be used to improve the measurement stability of POF-based BOCDR only when the spatial resolution is sufficiently low or when the incident power is sufficiently high. The threshold resolution and incident power should be dependent on other parameters, such as the sensing position and optical wavelength; therefore, further study is required on this point. We believe that these results will provide guidelines useful for the implementation of POF-based BOCDR systems with high measurement stabilities in long-term structural monitoring in the near future.

**Acknowledgments** This work was partially supported by Grants-in-Aid for Young Scientists (A) (No. 25709032) and for Challenging Exploratory Research (No. 26630180) from the Japan Society for the Promotion of Science (JSPS) and by research grants from the Iwatani Naoji Foundation, the SCAT Foundation, and the Konica Minolta Science and Technology Foundation. N. H. acknowledges a Grant-in-Aid for JSPS Fellows (No. 25007652).

- 1) G. P. Agrawal, *Nonlinear Fiber Optics* (Academic Press, San Diego, CA, 1995).
- 2) S. Norcia, S. Tonda-Goldstein, D. Dolfi, and J. P. Huignard, *Opt. Lett.* **28**, 1888 (2003).
- 3) Z. Zhu, D. J. Gauthier, and R. W. Boyd, *Science* **318**, 1748 (2007).
- 4) E. A. Kuzin, M. P. Petrov, and B. E. Davydenko, *Opt. Quantum Electron.* **17**, 393 (1985).
- 5) K. Y. Song, M. G. Herraes, and L. Thevenaz, *Opt. Express* **13**, 82 (2005).
- 6) T. Horiguchi and M. Tateda, *J. Lightwave Technol.* **7**, 1170 (1989).
- 7) T. Kurashima, T. Horiguchi, H. Izumita, and M. Tateda, *IEICE Trans. Commun.* **E76-B**, 382 (1993).
- 8) D. Garus, K. Krebber, and F. Schliep, *Opt. Lett.* **21**, 1402 (1996).
- 9) K. Hotate and T. Hasegawa, *IEICE Trans. Electron.* **E83-C**, 405 (2000).
- 10) Y. Mizuno, W. Zou, Z. He, and K. Hotate, *Opt. Express* **16**, 12148 (2008).
- 11) M. G. Kuzyk, *Polymer Fiber Optics, Materials, Physics, and Applications* (CRC Press, Boca Raton, FL, 2006).
- 12) Y. Koike and M. Asai, *NPG Asia Mater.* **1**, 22 (2009).
- 13) K. Nakamura, I. R. Husdi, and S. Ueha, *Proc. SPIE* **5855**, 807 (2005).
- 14) Y. Mizuno and K. Nakamura, *Appl. Phys. Lett.* **97**, 021103 (2010).
- 15) Y. Mizuno and K. Nakamura, *Opt. Lett.* **35**, 3985 (2010).
- 16) N. Hayashi, Y. Mizuno, and K. Nakamura, *Opt. Express* **20**, 21101 (2012).
- 17) N. Hayashi, K. Minakawa, Y. Mizuno, and K. Nakamura, *Appl. Phys. Lett.* **105**, 091113 (2014).
- 18) A. Minardo, R. Bernini, and L. Zeni, *IEEE Photonics Technol. Lett.* **26**, 387 (2013).
- 19) R. Bernini, A. Minardo, and L. Zeni, *IEEE Photonics J.* **4**, 48 (2012).
- 20) Y. Dong, P. Xu, H. Zhang, Z. Lu, L. Chen, and X. Bao, *Opt. Express* **22**, 26510 (2014).
- 21) N. Hayashi, Y. Mizuno, and K. Nakamura, *J. Lightwave Technol.* **32**, 3999 (2014).
- 22) R. Noe, H. J. Rodler, A. Ebberg, G. Gaukel, B. Noll, J. Wittmann, and F. Auracher, *J. Lightwave Technol.* **9**, 1353 (1991).
- 23) F. Bruyere, O. Audouin, V. Letellier, G. Bassier, and P. Marmier, *IEEE Photonics Technol. Lett.* **6**, 1153 (1994).
- 24) Y. Mizuno, Z. He, and K. Hotate, *Appl. Phys. Express* **2**, 062403 (2009).
- 25) Y. Mizuno, N. Hayashi, and K. Nakamura, *Electron. Lett.* **49**, 56 (2013).
- 26) Y. Mizuno, W. Zou, Z. He, and K. Hotate, *J. Lightwave Technol.* **28**, 3300 (2010).
- 27) K. Hotate and Z. He, *J. Lightwave Technol.* **24**, 2541 (2006).
- 28) C. Pulido and O. Esteban, *Sens. Actuators B* **157**, 560 (2011).
- 29) K. Minakawa, N. Hayashi, Y. Shinohara, M. Tahara, H. Hosoda, Y. Mizuno, and K. Nakamura, *Jpn. J. Appl. Phys.* **53**, 042502 (2014).